

Compact Asymmetric Coplanar Strip Fed MIMO Antenna with Band Dispersion Characteristics for UWB Applications

Bharghava Punna* and Pachiyaannan Muthusamy

Abstract—A MIMO antenna with ACS-asymmetric coplanar strip feeding technique with compact size for UWB applications of band-notched features is presented. The proposed MIMO antenna contains two orthogonally placed rectangular-shaped radiating elements. The orthogonal mechanism of placement of radiating elements provides a good amount of isolation from 3.09 GHz to 11.13 GHz. The size of the antenna is 27×27 mm². The isolation is more than 17 dB for most of the UWB range. The proposed MIMO antenna represents nearly omnidirectional radiation pattern and low value of envelope correlation coefficient. Because of the usage of ACS feeding techniques, the antenna size is reduced, and it is a uniplanar structure. The diversity performance of the MIMO antenna is explained in terms of ECC-Envelope Correlation Coefficient, DG-Diversity Gain, and TARC-Total Active Reflection coefficient.

1. INTRODUCTION

The ultra-wideband (UWB) antenna has two important and attractive properties, transmitting rate and cost. Transmitting rate is of high speed, and the cost is at a low value for UWB antenna. However, UWB antennas suffer from the problem of multipath fading in a highly dense medium because of reflections and diffractions. Multiple-input and multiple-output (MIMO) antenna has the efficiency for the mitigation of multipath fading. MIMO antenna with UWB nature has great attraction for researchers. In [1], a UWB-MIMO antenna is proposed with a tree-like structure for the provision of isolation. The MIMO antenna uses an orthogonal antenna layout and an open slot between the antennas to improve isolation as in [2]. In [3], a strip beneath the patch provides a good amount of isolation in MIMO antenna input ports. In [4], the F-shaped stubs are for less mutual coupling. The orthogonal placement of two radiators and protruding ground stubs provide less mutual coupling as given in [5]. In all above-mentioned papers, the feeding structure is a micro-strip line feeding technique. So the area occupied by the antenna is large. In [6], rectangular stubs and orthogonal placement of radiators are the reason for the good diversity performance, and Asymmetric Coplanar Strip (ACS) feeding mechanism is used to minimize the size of the antenna. In [7], less mutual coupling is obtained by arranging the antenna radiators with a large gap of distance, and an ACS based feeding technique is utilized. In [8], multiband characteristics are obtained using a monopole antenna structure, and ACS feed is taken for the radiator for giving the supply. In [9], an extended rectangular stub and orthogonality nature of the placement of radiators provide a decent quantity of isolation. The UWB-MIMO antenna is presented using the concept of fractal geometry. The self-similarity nature of fractal geometry is utilized to achieve larger impedance bandwidth as described in [10]. In [11], eight antennas of a dual-band 3.5/5.8 GHz MIMO radiator are used in an inverted F-shaped dual-band antenna. In [12], the ground plane is coupled to a Co-Planar Waveguide (CPW) supplied hexagonal ring antenna with monopole elements. In [13], a UWB-MIMO antenna uses a compact radiator to exhibit a number of stopbands. In [14], a Complementary Split

Received 8 July 2021, Accepted 6 August 2021, Scheduled 16 August 2021

* Corresponding author: Bharghava Punna (punnabharghava@gmail.com).

The authors are with the Advanced RF Microwave & Wireless Communication Laboratory, Vignan's Foundation for Science Technology and Research (Deemed to be University), Vadlamudi, Andhra Pradesh, India.

Ring Resonator (CSRR) UWB variant/MIMO antenna operating from 3 to 12 GHz is 82% efficient, the gain value 4.7 dBi, and the Envelope Correlation Coefficient (ECC) < 0.15 . In [15], the measurement of performance of 5G communication containing dual-mode and triple-band MIMO ten-antenna handset is observed with ECC-Envelope Correlation Coefficient ≤ 0.05 . In MIMO systems, isolation between radiators can be achieved by using L-shaped strips in the ground plane, and band notched characteristics can be obtained using L-shaped strips in the radiators. MIMO performance is measured in terms of ECC-Envelope Correlation Coefficient, Diversity Gain (DG), Total Active Reflection Coefficient (TARC) as mentioned in [16]. In [17], band notching characteristics are obtained by etching an inverted U-shaped slot in the middle portion of the radiating monopole antenna element.

This work presents an asymmetric coplanar strip-fed MIMO antenna of compactness with band-notched features. The proposed antenna is designed for the operation from 3.09 GHz to 11.13 GHz with two band notches 4.41 GHz to 5.71 GHz WLAN and lower X-band 7.96 GHz to 9.47 GHz. Without using any decoupling network, the proposed antenna has better isolation greater than 17 dB for most of the frequency band range. The design, simulation, fabrication, and measurement of the suggested antenna have been done. Commercial software Ansoft HFSS is used for the validation of the proposed antenna performance. The computer-generated and measured results are nearly identical. The MIMO antenna features are tested by evaluating ECC, DG, and TARC.

2. ACS FED MONOPOLE ANTENNA

In respect of compactness of the antenna, the feeding mechanism is very important. The feeding structure takes much of antenna size. The ACS-asymmetric coplanar strip fed antenna has advantages of uniplanar nature with compactness. The ACS feeding method is similar to the CPW feeding technique, but only one lateral ground strip is available in the ACS feed technique. Fig. 1 shows an ACS-fed monopole antenna. The commercially existing FR4 substrate is used for the fabrication of the antenna. FR4 material is with relative permittivity 4.4 and height 1.6 mm. The antenna size is very much reduced in comparison to the antenna with CPW feeding technique.



Figure 1. ACS fed monopole.

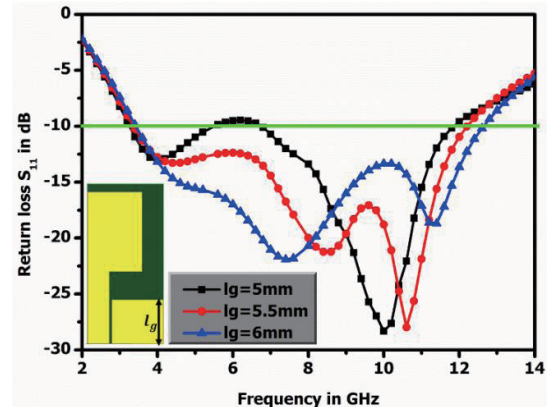


Figure 2. Return loss parametric variation of ACS fed monopole as length of ground varies as $l_g = 5$ mm, 5.5 mm and 6 mm.

The computer generated return loss features are specified in Fig. 2. From Fig. 2, it can be understood that for the ground length of 5 mm ultra-wideband is not generated and for the ground length of 5.5 mm the return loss is good in comparison to that of 6 mm. So in the proposed design, the length of ground is considered as 5.5 mm, and the antenna resonates from 3.32 GHz to 12.22 GHz for this ground length.

3. BAND NOTCH CHARACTERISTICS IN MONOPOLE ANTENNA

Using the current distribution, the location of slits should be identified. The frequency at which band notch is required decides the length of slit. In the monopole antenna designed, based on the current distribution two meandered strips are placed such that band notches have been obtained at WLAN and lower X-band. Fig. 3 represents current distribution on monopole patch at 5.5 GHz and 8.5 GHz. The slit dimensions are specified by quarter guided wavelength or half guided wavelength for both upper slit and lower slit currents and are calculated by the below mentioned equation as given in [16]

$$\text{Length of the slit} = \frac{c}{4f_{\text{notch}}\sqrt{\epsilon_e}} \tag{1}$$

It is taken by considering the notched frequency. The distribution of current is focused around upper and lower meandered slits at 5.5 GHz and 8.5 GHz, respectively. At different lengths of slits, parametric analysis is performed, and simulated results are given in Fig. 4. From Fig. 4 it is recognized that at the lengths of 10.9 mm for upper slit and 5.3 mm for lower slit, the slits provide sufficient notch bands in the impedance bandwidth. The return loss features of monopole antenna without slits and with slits are given in Fig. 5.

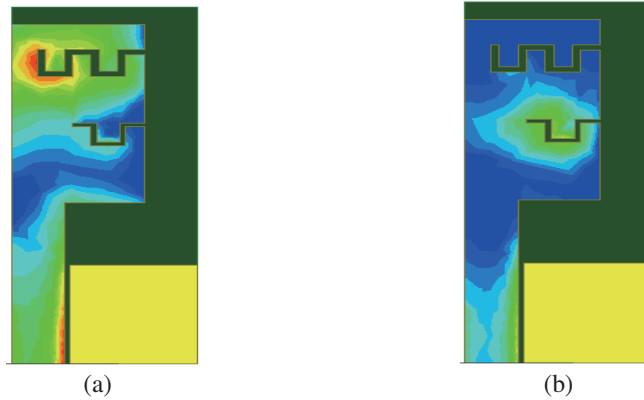


Figure 3. Current distribution on monopole radiator. (a) at 5.5 GHz, (b) at 8.5 GHz.

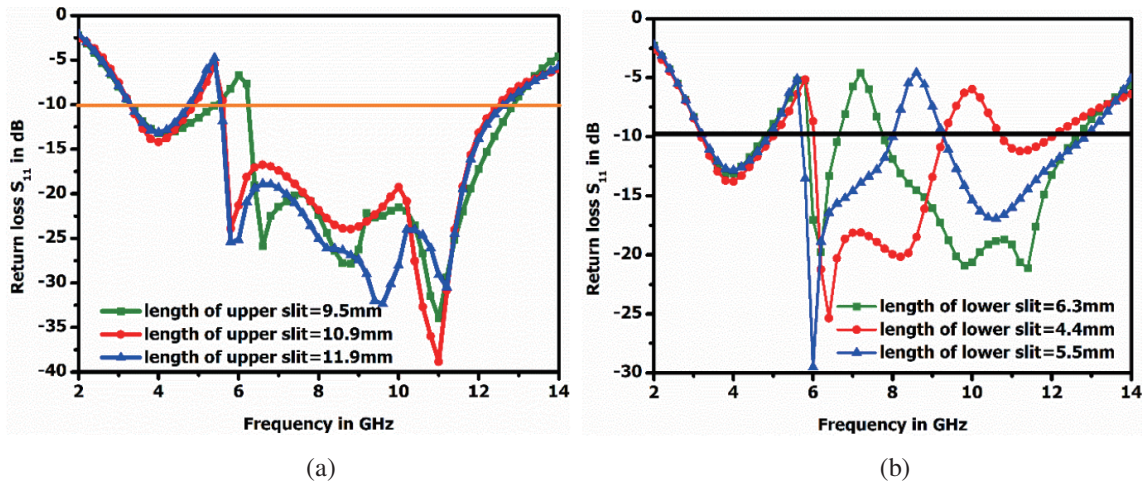


Figure 4. Return loss features of monopole as length of slit varies, (a) upper slit, (b) lower slit.

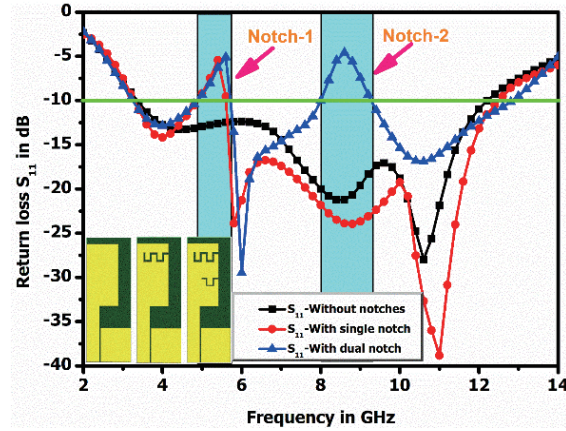


Figure 5. Return loss features for monopole without notches and with notches.

4. MIMO ANTENNA DESIGN

The proposed ACS fed MIMO antenna and its geometry with dual band-notched monopole antenna are presented in Fig. 6. The proposed antenna has very compact size $27 \times 27 \text{ mm}^2$. The commercially available FR4 material with a height of 1.6 mm and dielectric constant of 4.4 is used for the fabrication of proposed antenna. The suggested antenna comprises two ACS fed printed monopole antennas with band-notched slits denoted as ACSPM1 and ACSPM2, respectively. Fig. 6(b) represents ACSPM1 and ACSPM2.

The ACSPM1 and ACSPM2 are placed orthogonally to each other to maintain good amount of isolation between the two antenna input ports. The two ACS-fed rectangular-shaped radiators are placed on single side of dielectric material. The lateral ground planes of two ACS fed radiators are connected by ground strip to have common ground plane for ACSPM1 as well as ACSPM2. The optimization is carried out for the proposed antenna in terms of field pattern, impedance bandwidth, and gain with input signal at any one of the two excitation input ports and isolation available between two excitation ports. The geometrical dimensions of MIMO are given as listed in Table 1. The values in Table 1 are considered for the fabrication of the antenna given in Fig. 6(b).

As conveyed in Fig. 6(b), the suggested MIMO antenna has shorted the ground strip of width 1 mm

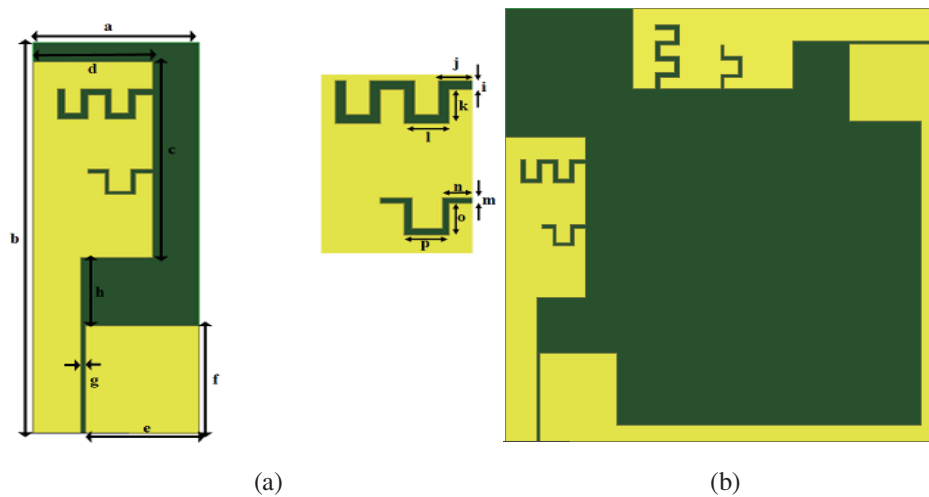


Figure 6. (a) Monopole with two slits along with dimensions, (b) ACS fed MIMO antenna.

which is considered to short the ground planes of two ACSPM radiators together. It is required to be considered as a single system. The orthogonal placement of two radiators is very essential for better isolation purpose. When the input impedance of one radiator is $50\ \Omega$ and other excited by input Fig. 7 represents the current distributions on ACSPM1 and ACSPM2. From Fig. 7, it is evident that isolation is obtained between two input ports.

Table 1. Measurements of proposed antenna.

Measurement	Value (mm)	Measurement	Value (mm)
<i>a</i>	7	<i>i</i>	0.3
<i>b</i>	20	<i>j</i>	1
<i>c</i>	10	<i>k</i>	1.2
<i>d</i>	5	<i>l</i>	1.3
<i>e</i>	4.8	<i>m</i>	0.2
<i>f</i>	5.5	<i>n</i>	0.9
<i>g</i>	0.2	<i>o</i>	1.1
<i>h</i>	3.5	<i>p</i>	1.3

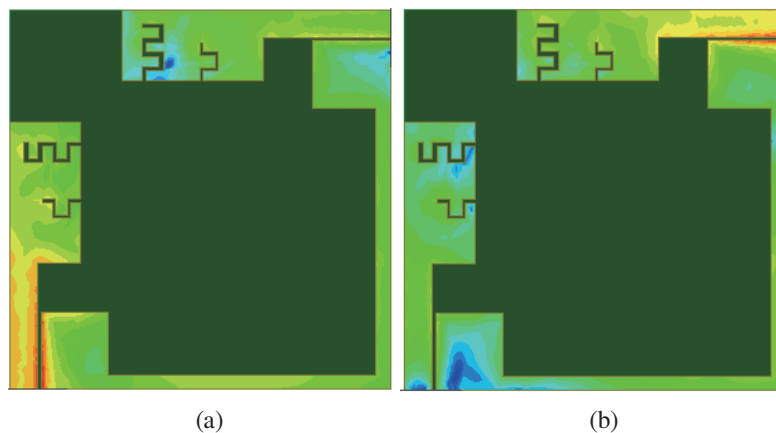


Figure 7. Current distribution on MIMO antenna when (a) port-1 is excited & port-2 is connected with $50\ \Omega$, (b) port-2 is excited & port-1 is connected with $50\ \Omega$.

5. RESULTS AND DISCUSSIONS

5.1. Scattering Parameters

By considering both computer-generated and measured results, S_{11} , S_{22} and S_{12} of the final proposed antenna are specified in Fig. 8. It is recognized from Fig. 8 that good agreement is available between computer-generated and measured outcomes. The obtained results after measurement in Fig. 8 give the information that input port is provided with impedance bandwidth from 3.08 GHz to 11.12 GHz for return loss less than $-10\ \text{dB}$. The isolation between two input ports is greater than 17 dB for most of the band and is considered for better performance. The differences observed between computer-generated and measured results are because of the effects of connectors taken in the measurement.

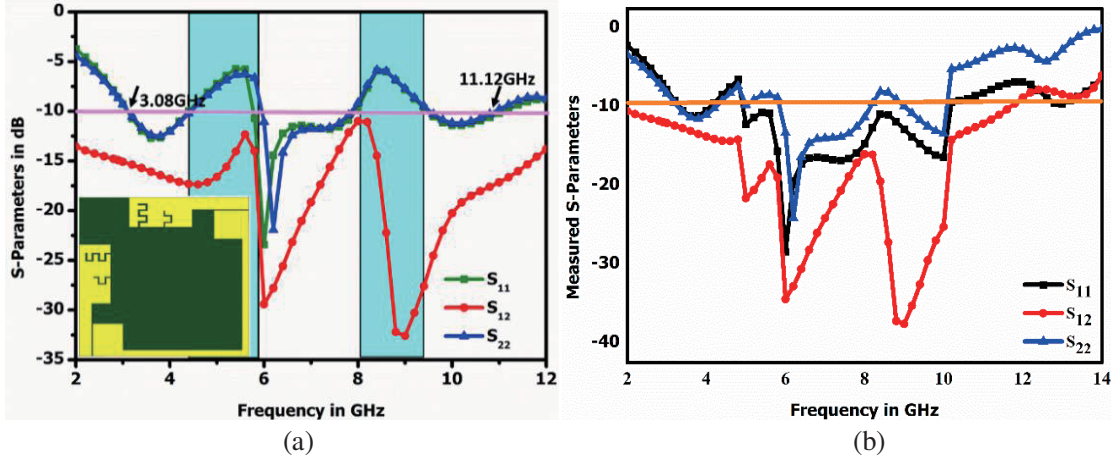


Figure 8. S -parameters of proposed MIMO antenna, (a) simulated results and (b) measured results.

5.2. Field Patterns

Figure 9 expresses the radiation patterns in 2-D form at 3.5 GHz, 7 GHz, and 10 GHz for the proposed antenna in XZ - and YZ -planes. When each antenna port is excited, maximum gain is 2.64 dB. In addition, Figs. 9(e) and 9(f) represent the deterioration of radiation pattern at higher frequencies because of splitting nature of the radiation lobes. The peak gain variation as a function frequency is shown in Fig. 10.

5.3. Diversity Analysis

The envelope correlation coefficient, total active reflection coefficient, and diversity gain are used to evaluate the proposed antenna's diversity. The envelope correlation coefficient of MIMO antenna is for the analysis of amount of correlation between adjacent radiating elements. The envelope correlation coefficient can be computed in terms of scattering parameters from below mentioned equation as given in [16].

$$\text{ECC} = \frac{|S_{11}^* S_{12} + S_{21}^* S_{22}|^2}{(1 - S_{11}^2 - S_{21}^2)(1 - S_{12}^2 - S_{22}^2)} \quad (2)$$

The value of ECC is ideally zero in the case of non-correlated MIMO antenna. The practical limit for ECC is < 0.5 . Fig. 11 represents the computer-generated ECC plot of the suggested MIMO antenna. The value of ECC of the suggested MIMO antenna is < 0.03 for most of the band. The computation of diversity gain of the recommended antenna is possible from below mentioned equation and is mentioned in [16].

$$\text{DG} = 10\sqrt{(1 - \text{ECC}^2)} \quad (3)$$

Figure 12 represents diversity gain of the recommended antenna using S -parameters, and the value of diversity gain is > 9.996 dB. The operating bandwidth and efficiency of the multipoint antenna are affected due to the affecting nature of adjacent radiating elements in the multipoint antenna system when operating simultaneously. So actual system behaviour cannot be predicted using only S -parameters. The TARC is the metric to take this effect into the consideration. TARC denotes the MIMO system's apparent return loss. As represented in [16] the TARC is computed by the below-mentioned equation in the case of 2-port MIMO system.

$$\text{TARC} = \sqrt{\frac{(s_{11} + s_{12})^2 + (s_{21} + s_{22})^2}{2}} \quad (4)$$

For the MIMO system, the desired value of TARC is 0 dB. The TARC of recommended MIMO antenna is depicted in Fig. 13. From Fig. 13, it is understood that the TARC for the antenna is less than -2.1 dB for the operating band of frequencies.

The fabricated proposed antenna is shown in Fig. 14. The comparison of various antennas with the proposed antenna is given in Table 2.

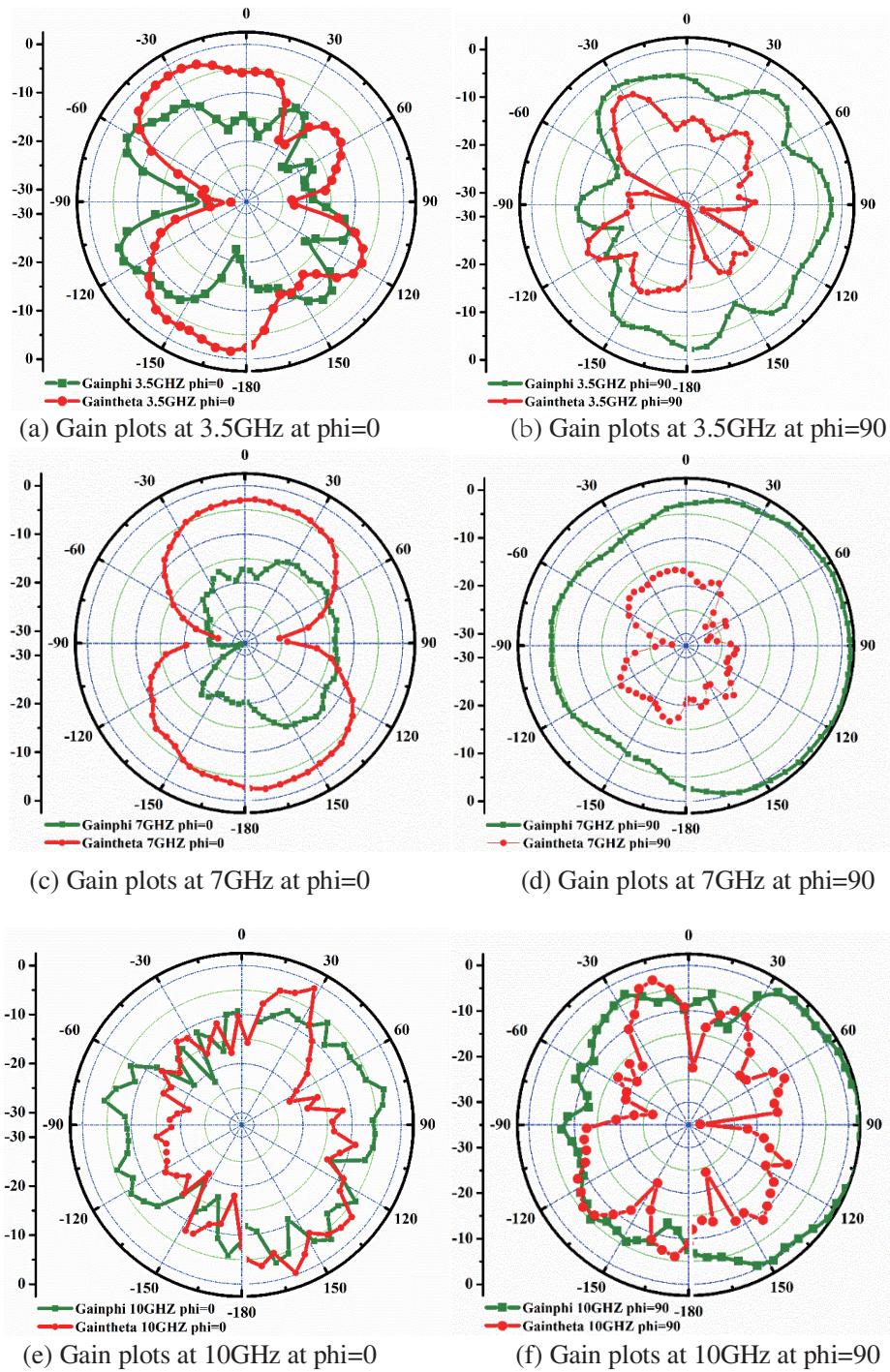
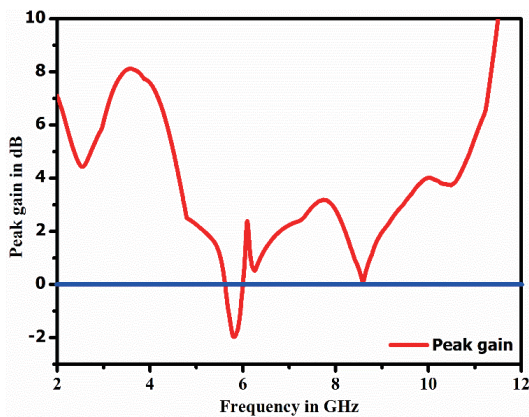
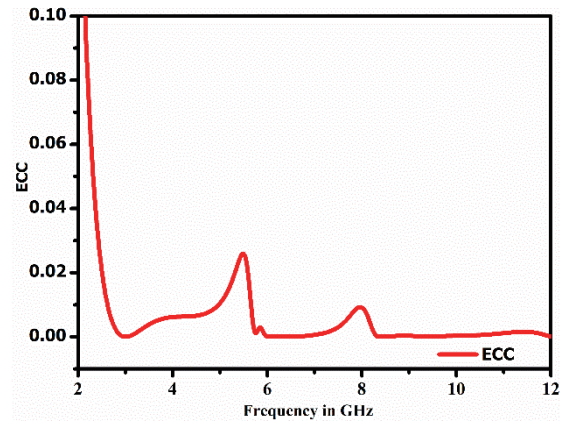


Figure 9. 2D gain plots at (a) 3.5 GHz $\phi = 0$, (b) 3.5 GHz $\phi = 90$, (c) 7 GHz $\phi = 0$, (d) 7 GHz $\phi = 90$, (e) 10 GHz $\phi = 0$, (f) 10 GHz $\phi = 90$.

Table 2. Comparison of various antennas.

Ref	Size (mm × mm)	IBW in GHz	Isolation in dB	Feeding technique	Gain in dB	ECC	Band notches
[1]	35 × 40	3.1–10.6	< -16	Microstrip line	6.5	< 0.01	-
[2]	32 × 32	3.1–10.6	< -15	Microstrip line	3.8	< 0.04	-
[3]	30 × 40	3.1–10.6	< -15	Microstrip line	4.2	< 0.05	WiMAX, WLAN
[4]	50 × 30	2.5–14.5	< -20	Microstrip line	4.3	< 0.04	-
[5]	26 × 40	3.1–10.6	< -15	Microstrip line	6.5	< 0.006	-
[6]	28.5 × 28.5	2.66–11.08	< -15	ACS feed	3.8	< 0.01	-
[7]	48 × 28	3–11.5	< -15	ACS feed	-	-	-
[8]	28 × 30	1.8, 2.4, 5.6 multiband	-	ACS feed	-	-	-
[9]	48 × 48	2.5–12	< -15	CPW feed	6	< 0.005	5.5 GHz, 4 GHz
[10]	24 × 32	3.1–12.5	< -16	Microstrip line	4	< 0.05	-
[11]	74 × 150	3.4–3.6 & 5.725–5.875	< -10	Microstrip line	-	< 0.15	-
[12]	45 × 25	3–12	< -20	CPW feed	5.4	< 0.2	-
[13]	27.2 × 46	3–17.6	< -18	Microstrip line	4	< 0.018	(2.5–3.57), (4.52–5.27), (6.91–8.91), (8.57–17.59)
[14]	23 × 29	3–12	< -15	Microstrip line	4.2	< 0.15	-
[16]	18 × 34	2.93–20	< -22	Microstrip line	7	< 0.01	(5.09–5.8), (6.3–7.27)
Proposed antenna	27 × 27	3.09–11.13	< -17	ACS feed	2.64	< 0.03	WLAN, Lower X-Band

**Figure 10.** Peak Gain of the antenna as change of frequency.**Figure 11.** ECC of proposed MIMO antenna.

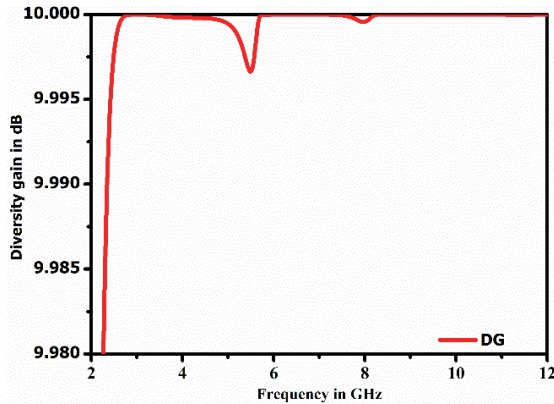


Figure 12. Diversity gain of proposed MIMO antenna.

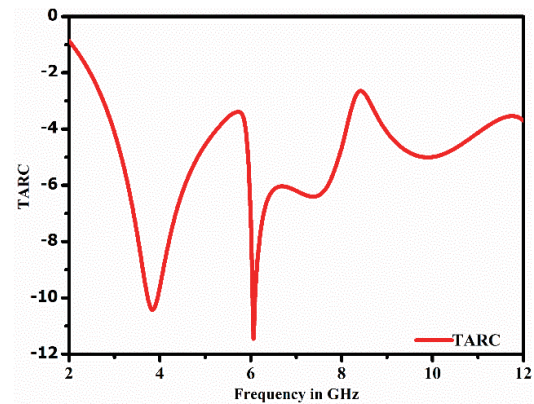


Figure 13. TARC of proposed MIMO antenna.

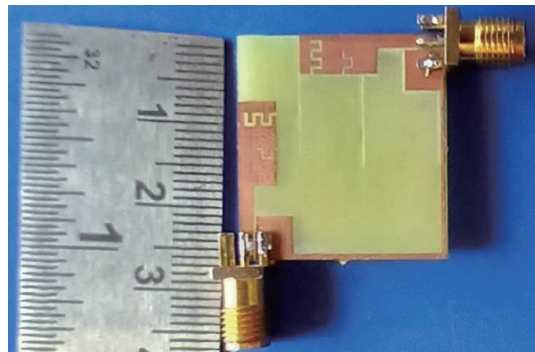


Figure 14. Photograph of proposed MIMO antenna.

6. CONCLUSION

In this study, a compact ACS-fed MIMO antenna with dual-band notch characteristics has been proposed for the application of UWB. The impedance bandwidth of the proposed monopole antenna is from 3.09 GHz to 11.13 GHz. The sufficient amount of isolation is obtained because of orthogonal placement, and even the radiators are kept on opposite faces of substrate. The isolation between the two ports is more than 17 dB for most of the impedance bandwidth. The max gain of the proposed antenna is 2.64 dB. The polarization diversity is ensured because of different linear polarizations due to radiators. The outcomes obtained from the diversity performance represent that the proposed antenna is suitable for MIMO applications.

ACKNOWLEDGMENT

We would like to acknowledge the Ansys software company and VFSTR (deem to be university), which has provided the Centre of Excellence (Keysight-Vignan's Advanced RF Microwave and Wireless Communications) resources.

REFERENCES

1. Zhang, S., Z. Ying, J. Xiong, and S. He, "Ultrawideband MIMO/diversity antennas with a tree-like structure to enhance wideband isolation," *IEEE Antennas and Wireless Propagation Letters*, Vol. 8, 1279–1282, 2009, doi: 10.1109/LAWP.2009.2037027.

2. Ren, J., W. Hu, Y. Yin, and R. Fan, "Compact printed MIMO antenna for UWB applications," *Antennas Wirel. Propag. Lett.*, Vol. 13, 1517–1520, 2014, doi: 10.1109/LAWP.2014.2343454.
3. Tang, T.-C. and K.-H. Lin, "An ultrawideband MIMO antenna with dual band-notched function," *IEEE Antennas and Wireless Propagation Letters*, Vol. 13, 1076–1079, 2014, doi: 10.1109/LAWP.2014.2329496.
4. Iqbal, A., O. A. Saraereh, A. W. Ahmad, and S. Bashir, "Mutual coupling reduction using F-shaped stubs in UWB-MIMO antenna," *IEEE Access*, Vol. 6, 2755–2759, 2018, doi: 10.1109/ACCESS.2017.2785232.
5. Liu, L., S. W. Cheung, and T. I. Yuk, "Compact MIMO antenna for portable devices in UWB applications," *IEEE Trans. Antennas Propagat.*, Vol. 61, No. 8, 4257–4264, Aug. 2013, doi: 10.1109/TAP.2013.2263277.
6. Liu, Y., P. Wang, and H. Qin, "Compact ACS-fed UWB antenna for diversity applications," *Electron. Lett.*, Vol. 50, No. 19, 1336–1338, Sep. 2014, doi: 10.1049/el.2014.1678.
7. Ibrahim, A. A., J. Machac, R. M. Shubair, and M. Svanda, "Compact UWB MIMO antenna with asymmetric coplanar strip feeding configuration," *2017 IEEE 28th Annual International Symposium on Personal, Indoor, and Mobile Radio Communications (PIMRC)*, 1–4, Oct. 2017, doi: 10.1109/PIMRC.2017.8292768.
8. Deepu, V., R. K. Raj, M. Joseph, M. N. Suma, and P. Mohanan, "Compact asymmetric coplanar strip fed monopole antenna for multiband applications," *IEEE Transactions on Antennas and Propagation*, Vol. 55, No. 8, 2351–2357, Aug. 2007, doi: 10.1109/TAP.2007.901847.
9. Gao, P., S. He, X. Wei, Z. Xu, N. Wang, and Y. Zheng, "Compact printed UWB diversity slot antenna with 5.5-GHz band-notched characteristics," *IEEE Antennas and Wireless Propagation Letters*, Vol. 13, 376–379, 2014, doi: 10.1109/LAWP.2014.2305772.
10. Gurjar, R., D. K. Upadhyay, B. K. Kanaujia, and K. Sharma, "A novel compact self-similar fractal UWB MIMO antenna," *Int. J RF Microw. Comput. Aided Eng.*, Vol. 29, No. 3, e21632, Mar. 2019, doi: 10.1002/mmce.21632.
11. Wong, K.-L., B.-W. Lin, and B. W.-Y. Li, "Dual-band dual inverted-F/loop antennas as a compact decoupled building block for forming eight 3.5/5.8-GHz MIMO antennas in the future smartphone," *Microw. Opt. Technol. Lett.*, Vol. 59, No. 11, 2715–2721, Nov. 2017, doi: 10.1002/mop.30811.
12. Mathur, R. and S. Dwari, "Compact CPW-fed ultrawideband MIMO antenna using hexagonal ring monopole antenna elements," *AEU — International Journal of Electronics and Communications*, Vol. 93, 1–6, Sep. 2018, doi: 10.1016/j.aeue.2018.05.032.
13. Dabas, T., D. Gangwar, B. K. Kanaujia, and A. K. Gautam, "Mutual coupling reduction between elements of UWB MIMO antenna using small size uniplanar EBG exhibiting multiple stop bands," *AEU — International Journal of Electronics and Communications*, Vol. 93, 32–38, Sep. 2018, doi: 10.1016/j.aeue.2018.05.033.
14. Khan, M. S., A.-D. Capobianco, S. M. Asif, D. E. Anagnostou, R. M. Shubair, and B. D. Braaten, "A compact CSRR-enabled UWB diversity antenna," *Antennas Wirel. Propag. Lett.*, Vol. 16, 808–812, 2017, doi: 10.1109/LAWP.2016.2604843.
15. Li, Y. and G. Yang, "Dual-mode and triple-band 10-antenna handset array and its multiple-input multiple-output performance evaluation in 5G," *Int. J RF Microw. Comput. Aided Eng.*, e21538, Dec. 2018, doi: 10.1002/mmce.21538.
16. Chandel, R., A. K. Gautam, and K. Rambabu, "Tapered fed compact UWB MIMO-diversity antenna with dual band-notched characteristics," *IEEE Transactions on Antennas and Propagation*, Vol. 66, No. 4, 1677–1684, Apr. 2018, doi: 10.1109/TAP.2018.2803134.
17. Chung, K., J. Kim, and J. Choi, "Wideband microstrip-fed monopole antenna having frequency band-notch function," *IEEE Microwave and Wireless Components Letters*, Vol. 15, No. 11, 766–768, Nov. 2005, doi: 10.1109/LMWC.2005.858969.